

Doubly resonant WW plus jet signatures at the LHC

Johan Alwall,^{1,*} Tsedenbaljir Enkhbat,^{1,†} Wei-Shu Hou,^{2,‡} and Hiroshi Yokoya^{1,3,§}

¹*Department of Physics and Center for Theoretical Sciences,*

National Taiwan University, Taipei 10617, Taiwan

²*Department of Physics, National Taiwan University, Taipei 10617, Taiwan*

³*National Center for Theoretical Sciences,*

National Taiwan University, Taipei 10617, Taiwan

Abstract

We present search prospects and phenomenology of doubly resonant signals that come from the decay of a neutral weak-singlet color-octet vector state ω_8 into a lighter weak-triplet color-octet scalar π_8 , which can arise in several theories beyond the Standard Model. Taking $m_{\omega_8} - m_{\pi_8} > m_W$, we demonstrate an analysis of the signals $pp \rightarrow \omega_8 \rightarrow \pi_8^\pm W^\mp (\pi_8^0 Z) \rightarrow gW^\pm W^\mp (gZZ)$. The present 8 TeV LHC run is found to have the potential to exclude or discover the signal for a range of masses and parameters. The preferred search channel has a boosted W -tagged jet forming a resonance with a second hard jet, in association with a lepton and missing energy.

PACS numbers: 14.40.Rt, 13.25.Jx, 13.38.Be, 13.85.Rm

*Electronic address: jalwall@ntu.edu.tw

†Electronic address: enkhbat@phys.ntu.edu.tw

‡Electronic address: wshou@phys.ntu.edu.tw

§Electronic address: hyokoya@hep1.phys.ntu.edu.tw

I. INTRODUCTION

The LHC experiments are now collecting data at an unprecedented rate, bringing in an exciting period for potential new discoveries. As a hadron collider, it is particularly apt at probing for new colored objects. Such particles are predicted in a variety of theories beyond the Standard Model (SM), and include: massive gluons [1, 2] including KK gluon [3–5], diquarks [6], leptoquarks [6, 7], excited quarks [8, 9], squarks and gluino [10], colored version of technicolor particles [11] and other composite colored objects [12–21]. Currently, many of these objects have been searched for by the CMS and ATLAS collaborations at the LHC, with lower bounds [22–27] placed on their masses. Among composite colored objects, a neutral $SU(2)_L$ singlet color-octet vector resonance, as predicted by many models [1, 3, 4, 12–16], is of particular interest, since it can be produced singly. These objects often cascade decay to other lower lying states, leading to distinct collider signals. With masses in the TeV range, they often lead to boosted t 's and W 's in the final states. The study of such cascade decays is important in its own right, since it differs characteristically from studies for a single resonance decaying to a pair of light SM particles. Whatever beyond the SM physics we consider, it often contains not just one but multiple particles with various different quantum numbers, and may lead to a double resonant signal.

In the current study, we examine the phenomenology of an $SU(2)_L$ singlet color-octet vector particle accompanied by a lighter $SU(2)_L$ triplet color-octet scalar. The weak $SU(2)_L$ quantum number, as an isospin symmetry, often plays a crucial role for classifying possible spectrum. A prevailing feature among many dynamical electroweak symmetry breaking models is that they have isotriplets as the lower lying states, accompanied by heavier isosinglets. For example technicolor models, whether $SU(3)_c$ colored versions or not, have spectra with π and ρ -like resonances as the lightest states, followed by an ω -like resonance. This spectrum also naturally arises when considering states composed of a pair of $SU(2)_L$ doublet color-triplet spin-half particles, such as the scenario studied in Ref. [16].

As a case study for a signal that has not been considered previously, and as an excellent example of a signal that can naturally appear when studying resonant structures with more than one colored state, we consider $\omega_8 \rightarrow \pi_8 W/Z$ followed by $\pi_8 \rightarrow gW/Z$, assuming $m_{\omega_8} - m_{\pi_8} > M_W$. While such spectrum has appeared in several scenarios beyond the SM, phenomenological studies thus far have been restricted to one resonance at a time [4, 8, 11, 14, 18, 20]. Thus, the final decay products we consider are $\omega_8 \rightarrow (\pi_8^\pm W^\mp, \pi_8^0 Z) \rightarrow (gW^\pm W^\mp, gZZ)$. With the ω_8 mass in the TeV range and a π_8 mass of several hundred GeV, this decay chain leads to a spectacular signal with a very energetic

hadronic jet and at least one highly boosted W or Z boson. To take full advantage of the presence of such boosted objects in our signal, we employ techniques for tagging boosted objects using jet substructure [28–30]. This also allows for an excellent reconstruction of the invariant mass of such objects, once they have been discovered.

The paper is organized as follows. In Section II, we give the details about the signature, and discuss the methods we use for tagging boosted weak bosons that decay hadronically, and for determining exclusion and discovery limits. Details of the numerical simulation and results are given in Section III, and in Section IV, we give conclusions and discussion.

II. MODEL SETUP AND COLLIDER SIGNATURES

The scenario we consider has an $SU(2)_L$ singlet color-octet vector boson ω_8 that decays to an $SU(2)_L$ triplet color-octet scalar boson π_8 plus an $SU(2)_L$ gauge boson. The π_8 boson subsequently decays to a gluon and another weak boson, leading to a doubly resonant signal $W^\pm(W^\mp + \text{jet})$ or $Z(Z + \text{jet})$. While additional color-singlet states might be present in the spectrum depending on the details of the model, we disregard them in this study, since the production cross section of such color-singlet particles typically would be considerably smaller than that of the states discussed here.

Note that single production of π_8 from gluon fusion is forbidden by its isotriplet nature. Although in principle $q\bar{q}$ initial states can be allowed, they, and the corresponding dijet decays, are usually suppressed in dynamical models. This is because the couplings to the light generations are usually proportional to the Yukawa couplings since the color-singlet counter parts are the Goldstone bosons. This still leaves the possibility of decay to $t\bar{t}$. However, inducing a large enough top Yukawa coupling in these models is usually problematic and often invokes some extra mechanism. We here ignore this possibility and restrict our phenomenological study to $\pi_8 \rightarrow Wg$, which should always be present based on quantum numbers alone. This decay also naturally appears in composite models such as the one studied in Ref. [16].

The ω_8 on the other hand is an $SU(2)_L$ singlet vector boson, and can be produced singly in $q\bar{q}$ fusion (gluon fusion production is forbidden by Yang’s theorem [31]). Therefore at hadron colliders, the leading production mechanism of new states in this scenario, for sufficiently heavy π_8 , is single ω_8 production via quark anti-quark annihilation, $q\bar{q} \rightarrow \omega_8$. The corresponding Feynman diagram is drawn in Fig. 1.

Besides the decay $\omega_8 \rightarrow \pi_8 W/Z$, ω_8 can also decay to $q\bar{q}$ ($t\bar{t}$), as required by the unitarity

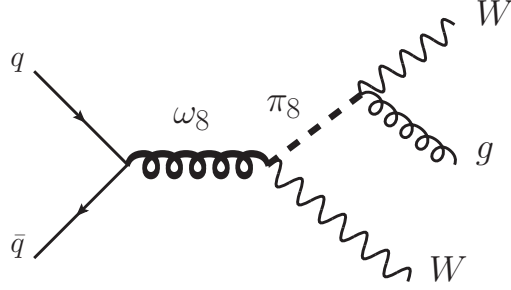


FIG. 1: Feynman diagram of the $q\bar{q} \rightarrow \omega_8 \rightarrow \pi_8 W \rightarrow gWW$ process.

relation. Thus the interactions that give the leading decays are expressed by the following effective operators:

$$\begin{aligned} \mathcal{L}_{\omega_8\text{-decay}} = & \xi \frac{g_s}{\sqrt{2}} \bar{q}_i \gamma_\mu (T^a)_{ij} q_j V_a^\mu + \frac{gW}{\sqrt{m_S m_V}} [f_v \epsilon^{\mu\nu\rho\sigma} (\partial_\sigma S_a^\pm \partial_\rho W_\mu^\mp + \partial_\sigma S_a^0 \partial_\rho Z_\mu) V_{a\nu} \\ & + S_a^\pm (f_{a_1} m_S m_V V_a^\mu + f_{a_2} \partial^\mu V_{a\nu} \partial^\nu + f_{a_3} V_{a\nu} \partial^\mu \partial^\nu) W_\mu^\mp \\ & + S_a^0 (f_{a_1} m_S m_V V_a^\mu + f_{a_2} \partial^\mu V_{a\nu} \partial^\nu + f_{a_3} V_{a\nu} \partial^\mu \partial^\nu) Z_\mu] . \end{aligned} \quad (1)$$

where $\xi \equiv f_V/m_V$ is the decay constant (in units of m_V) for the color-octet vector V , f_v and f_{a_i} are form factors for the effective operators connecting V with the $SU(2)_L$ triplet color-octet scalar S . Note that $SU(2)_L$ indices have been suppressed. The decay constant parameter ξ fixes the production cross-section and the dijet rate. The form factors f_{v,a_i} control the transition decay of ω_8 to π_8 's. In the analysis given in the next Section, we assume that f_{v,a_i} are large enough compared to ξ for the decay into $\pi_8 W/Z$ to dominate over the dijet decay. Note that isospin invariance fixes the ratio of $\mathcal{B}(\omega_8 \rightarrow \pi_8^0 Z)/\mathcal{B}(\omega_8 \rightarrow \pi_8^\pm W^\mp)$ to be 1 : 2, where we ignore the W and Z mass difference.

If ξ is large enough relative to f_{v,a_i} to get a significant branching ratio into $q\bar{q}$, the value of ξ can be constrained by the dijet resonance searches. Stringent limits on the high-mass dijet resonance production cross-section have been obtained by CMS with 5 fb⁻¹ data [22]. We convert this limit into an upper limit for ξ by using the first term of Eq. (1) to calculate the single ω_8 cross-section at the LHC. The partonic cross-section for this process can be written as [16]

$$\hat{\sigma}_{q\bar{q} \rightarrow \omega_8}(\hat{s}) = \frac{32\pi^3 \alpha_s^2}{9m_{\omega_8}^2} \xi^2 \delta(1 - m_{\omega_8}^2/\hat{s}). \quad (2)$$

Assuming the 100% branching ratio of ω_8 into dijet, ξ is constrained to be less than ~ 0.1 (~ 0.2) for $m_{\omega_8} = 1000$ (2000) GeV. However, if the branching ratio into dijet is assumed to be small, the limit is considerably weakened.

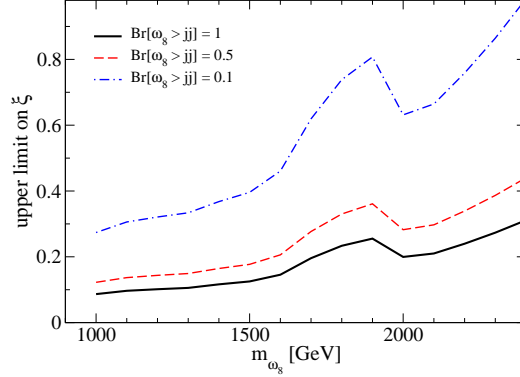


FIG. 2: Upper limit on $\xi = f_{\omega_8}/m_{\omega_8}$ from the CMS dijet resonance search with $\mathcal{L} = 5 \text{ fb}^{-1}$ [22]. Several lines correspond to different assumptions of the branching ratio of ω_8 into dijet.

In Fig. 2, we plot the upper limit on ξ obtained from the CMS dijet data with 5 fb^{-1} [22] by assuming several values of the branching ratio of ω_8 into dijet. To calculate the hadronic cross-section at the LHC, we have used the CTEQ6L1 parton distribution functions [32] with the factorizing scale $\mu_F = m_{\omega_8}$. It is clear that, so long that the dijet does not dominate ω_8 decay, the bound on ξ is very accommodating. This illustrates the importance for resonances searches beyond the simple dijet decays.

In our analysis, we assume that the π_8 has a mass above 600 GeV, for several reasons: If the π_8 is light, it would have a large $gg \rightarrow \pi_8 \bar{\pi}_8$ pair production cross section at the LHC, leading to a different phenomenology [17, 19] than we are considering here. Furthermore, we want to consider the region where the W/Z from the π_8 decay is sufficiently boosted for W -jet tagging to be effective.

A. Collider signatures

The W - (Z -) boson from π_8 decay is expected to be very energetic, since the energy is half the resonance mass in the π_8 rest-frame. On the other hand, the energy of the W - (Z -) boson of the ω_8 decay is characterized by the mass difference between the two states. For composite particles, we can expect the mass splitting to be considerably smaller than the mass of each of the states. The WWg (ZZg) signal in this case has one hard vector boson with energy of order half the resonance mass, and one soft vector boson with energy characterized by the mass difference between the resonances. Although in the next Section, we extend our analysis to allow for a free mass ratio between the new states, we will in the following refer to the W (Z) from the π_8 decay as the “hard” vector boson, and that from the ω_8 decay as the “soft” vector boson.

We first consider the case when $\omega_8 \rightarrow \pi_8^\pm W^\mp$. When both W -bosons decay hadronically, it

is difficult to distinguish the signal from the large QCD multijet background. The semi-leptonic decay is more promising, due to the presence of an isolated lepton and missing energy, which significantly reduces the background. It has two cases: The hard W decays hadronically while the soft W decays leptonically, where we consider only decays to e and μ , and vice versa. The former case has an isolated charged lepton plus sizable missing transverse momentum with three energetic jets, two of which are highly collimated due to the large boost of the W . In this case, it is useful to analyze the hadronically decaying W as a single “fat” jet with a substructure of two “subjets”. Some methods for doing this will be discussed in Sec. II B below. The latter case is characterized by a highly energetic isolated charged lepton plus large missing transverse momentum, one very energetic jet and two more jets which have an invariant-mass close to m_W . Due to the large boost, the directions of the charged lepton and the missing transverse momentum in the transverse plane are close to each other.

Finally, dileptonic decay $WWg \rightarrow (\ell\nu)(\ell\nu)j$ would be seen as two charged leptons plus large missing transverse momentum and one very energetic jet. The dileptonic decay ratio into e and μ is only about 5%, so too small to be interesting in a discovery study. Furthermore, the reconstruction of the final state is more difficult in the dilepton case.

We next consider the decay of ω_8 into a neutral π_8^0 plus a Z boson, giving a final state of ZZg . The semileptonic cases are $ZZg \rightarrow (\ell^+\ell^-)(jj)j$ and $(jj)(\ell^+\ell^-)j$, where the first (second) parenthesis denotes the decay of the soft (hard) Z -boson. In the case where the hard Z -boson decays leptonically, the leptons are highly collimated, therefore only the muonic decay may possibly be measured with some precision. In the case of hadronic decay of the hard Z boson, the dijet will again be collimated, and the methods discussed in Sec. II B below can be used. In order to reduce the large backgrounds from dileptonic $t\bar{t}$ decay, the analysis in Sec. III requires the dilepton invariant mass to be close to m_Z , and the missing energy to be small.

In Sec. III, we will perform a detailed analysis of these collider signatures.

B. W -jet tagging

We explain here the W -tagging method used in our study. We follow the method laid out in Ref. [33]. Similar detailed studies can be found e.g. in Refs. [29, 34]. According to Ref. [33], the W -tagging method is summarized as follows:

1. Find jets by the C/A algorithm with $R = 0.8$; keep the clustering history and momenta of clusters to be merged at each step.

2. Perform pruning [35]: Rerun the clustering; at each step, check if the two clusters a and b satisfy the two conditions,

$$z_{ab} \equiv \frac{\min(p_T^a, p_T^b)}{p_T^J} < z_{\text{cut}}, \quad (3)$$

$$\Delta R_{ab} > D_{\text{cut}} \equiv \alpha \cdot \frac{M_J}{p_T^J}, \quad (4)$$

where $\Delta R_{ab} = \sqrt{(\Delta\eta_{ab})^2 + (\Delta\phi_{ab})^2}$ and M_J is the mass of the jet in the original clustering sequence. If so, throw away the softer cluster instead of merging. The default values [35] $z_{\text{cut}} = 0.1$ and $\alpha = 1$ are taken for the pruning parameters.

3. Mass drop tagging [28]: Require the pruned jet mass to satisfy $60 \text{ GeV} < M_{\text{jet}} < 100 \text{ GeV}$; the jet is tagged as a W candidate if there exists a mass drop,

$$\frac{M_1}{M_{\text{jet}}} < 0.4, \quad (5)$$

where M_1 is the mass of the hardest cluster in the last step of the pruning procedure.

C. The CL_s method

In the analysis described in the following section, we use the CL_s method [36] to determine the expected cross section exclusion and discovery prospects at the 20 fb^{-1} early LHC run of 2012. The CL_s method was developed for Higgs searches by the LEP experiments, and it is the standard method used for determining exclusion limits at the LHC. The fundamental quantity used to determine the exclusion level is

$$\text{CL}_s \equiv \text{CL}_{s+b} / \text{CL}_b \quad (6)$$

where $\text{CL}_{s+b} = P_{s+b}(Q \leq Q_{\text{obs}})$ and $\text{CL}_b = P_b(Q \leq Q_{\text{obs}})$ are the probabilities for some test-statistic to be less than or equal to the observed value. This definition allows for a consistent frequentist statistical treatment of experimental results in the presence of backgrounds. An exclusion at confidence level CL is reached when $1 - \text{CL}_s \leq \text{CL}$.

As test-statistic, we use the likelihood ratio $Q = \mathcal{L}(\vec{X}, s+b) / \mathcal{L}(\vec{X}, b)$ for a given experimental result \vec{X} . For a result presented as a binned histogram with N_{chan} bins, this likelihood ratio can be expressed as

$$Q = e^{-s_{\text{tot}}} + \prod_{k=1}^{N_{\text{chan}}} \left(1 + \frac{s_i}{b_i}\right)^{n_i} \quad (7)$$

Here, s_{tot} is the total signal rate for all channels, s_i and b_i are the number of signal and background events in bin i , and n_i is the number of observed events in bin i .

The probability distributions $P_{s+b}(Q \leq Q_{\text{obs}})$ and $P_b(Q \leq Q_{\text{obs}})$ are determined using test experiments starting from signal and background histograms with associated statistical and systematic uncertainties. To do this, and to determine the resulting expected exclusion limits, we use the RooStat package [37]. Besides the statistical uncertainty from the Monte Carlo statistics and expected event statistics, we also assume a 20% systematic uncertainty on the SM backgrounds.

For a discovery analysis, the procedure is the same, except CL_{s+b} is used instead of CL_s .

III. NUMERICAL SIMULATIONS AND RESULTS

For the numerical analysis of the signatures described in the previous sections, we simulate both signal and the SM backgrounds using MadGraph 5 [38] interfaced with PYTHIA 6.4 [39] for hadronization and underlying event, and Delphes 1.9.2 [40] for detector simulation. The signal model is implemented directly in the UFO format [41]. Both signal and backgrounds are simulated using the jet matching techniques described in Ref. [42]. For the detector simulation, the CMS card included in the MadGraph distribution is employed with the modification that the jet reconstruction scheme used is anti- k_T [43] and the jet radius is set to 0.4. W -tagged jets are reconstructed by using FastJet [44] starting from the calorimetric clusters in Delphes by the method described in the previous section, and anti- k_T jets corresponding to such jets are removed from the hard jet list. As a crosscheck, both simulations and analyses are done independently by two of us using two independent analysis programs.

Since the different signatures have quite different properties, we will go through them in sequence in the following.

A. Hard W -tagged jet with soft leptonic W

The first, and most promising, decay mode that we analyze is $\omega_8 \rightarrow \pi_8^\pm (W^\mp)_{\text{leptonic}}$ with $\pi_8^\pm \rightarrow (W^\pm)_{\text{hadronic}} + \text{jet}$, where “leptonic” includes decays to e^\pm and μ^\pm . In this decay mode, we have a lepton and missing energy giving excellent trigger and QCD multijet background separation. The hadronic decay products of the W^\pm from π_8 decay are collimated and can be analyzed as a W jet, as described in section II B. Note that, in our analysis we do not make any stringent assumption regarding the ω_8 - π_8 mass splitting, except that it is larger than the W mass.

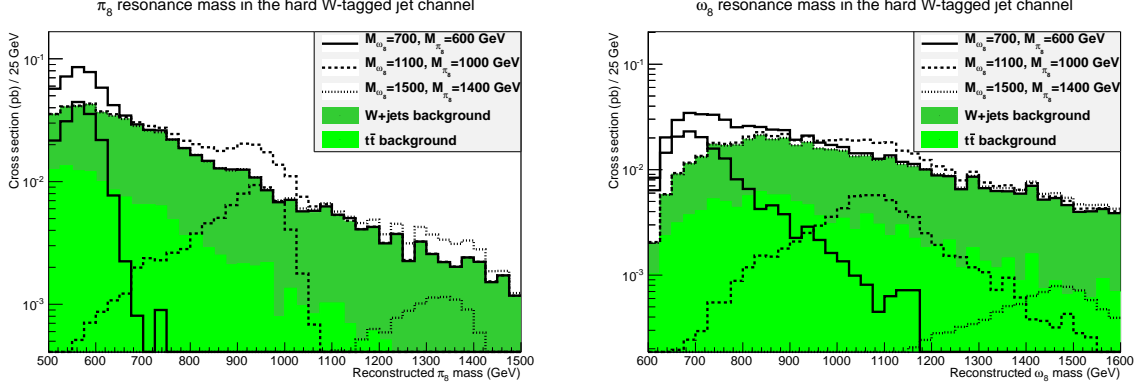


FIG. 3: Invariant mass distributions for the reconstructed π_8 and ω_8 for a few sample mass points in the hard W -tagged jet channel (see the text for details). The ω_8 decay constant ξ parameter is set to 0.2, in order to make the curves clearly distinguishable on top of the backgrounds.

The main SM backgrounds for this signature are W^\pm associated with hard QCD radiation faking a W jet, and semi-leptonically decaying $t\bar{t}$, where the W jet comes from either a boosted hadronically decaying W or is being faked by a hard b jet. The irreducible background W^\pm in association with a W or Z boson and jets is only a few % of the main backgrounds.

We use the following set of cuts for our event selection:

- Exactly 1 isolated lepton (e or μ) with $p_\perp > 20$ GeV;
- Missing $E_T > 20$ GeV;
- A W -tagged jet j_W with $p_\perp > 200$ GeV;
- A jet j_1 with $p_\perp > 200$ GeV;
- Invariant mass (reconstructed π_8 mass) $M(j_W, j_1) > 500$ GeV.

Varying the jet p_\perp cuts only has a minimal effect on the resulting exclusion curves.

The reconstructed π_8 and ω_8 masses are shown for a few different $(m_{\omega_8}, m_{\pi_8})$ mass points in Fig. 3, together with the main backgrounds. We use $\xi = 0.2$ in the figure, to make the curves easily visible on top of the background. Note that the cross section scales as ξ^2 , since we assume 100% branching fraction into the π_8 and a weak boson final state. The width of the invariant mass distributions is mainly due to the relatively large energy scale uncertainties for the reconstructed W jet, and the jet energy scale uncertainty for the gluon jet. To reconstruct the ω_8 mass, we first need to perform leptonic W reconstruction. In the reconstruction of the leptonic W , we pick the

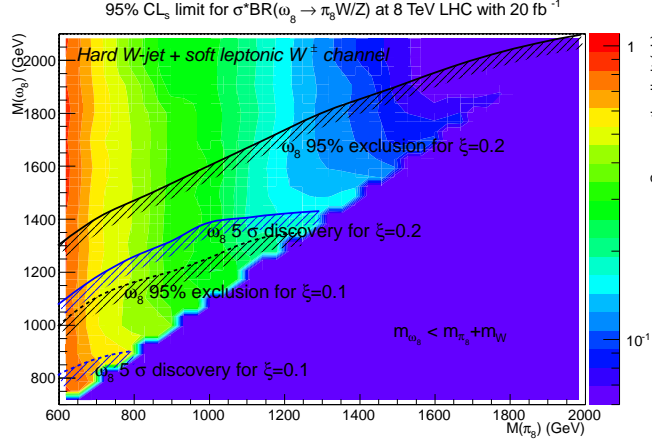


FIG. 4: Cross section exclusion limits in pb in the (ω_8, π_8) mass plane in the hard W -tagged jet channel, for 20 fb^{-1} integrated luminosity at the 8 TeV LHC. Also the exclusion regions for ω_8 with ξ set to 0.1 and 0.2 are indicated.

solution with the smallest neutrino z momentum. We furthermore allow a reconstructed W mass up to 100 GeV, and if necessary adjust the magnitude of the missing E_T to bring the W mass back to the nominal value.

In the exclusion and discovery analysis, we use the reconstructed π_8 mass, since the peak resolution of the π_8 is considerably better than the ω_8 case. Note however that the double-resonant assumption is crucial for the background suppression as described above.

In Fig. 4 we give the 95% C.L. cross section exclusion contours for 20 fb^{-1} at the 8 TeV LHC, using the CL_s method as discussed in Sec. II C. We also show both the exclusion as well as 5σ discovery limits for ω_8 production for two different values of ξ , 0.1 and 0.2, assuming $\mathcal{B}(\omega_8 \rightarrow \pi_8^\pm W^\mp) = 2/3$ and $\mathcal{B}(\omega_8 \rightarrow \pi_8^0 Z) = 1/3$, and $\pi_8^\pm \rightarrow W + \text{jet}$ decay 100% of the time. For ω_8 and π_8 mass difference close to m_W , the LHC will be able to exclude ω_8 production up to 2100 GeV (1350 GeV) for $\xi = 0.2$ (0.1) with 20 fb^{-1} integrated luminosity, and make an ω_8 discovery for masses up to 1400 GeV (900 GeV) for $\xi = 0.2$ (0.1).

B. Hard leptonic W and soft hadronic W

The next decay mode we consider is $\omega_8 \rightarrow \pi_8^\pm (W^\mp)_{\text{hadronic}}$ with $\pi_8^\pm \rightarrow (W^\pm)_{\text{leptonic}} + \text{jet}$, where “leptonic” again includes decays to e^\pm and μ^\pm only. While this decay mode has exactly the same branching ratio suppression as the previously discussed “hard W jet mode”, it lacks the distinguishing W jet signature. On the other hand, it requires two jets in the event to reconstruct

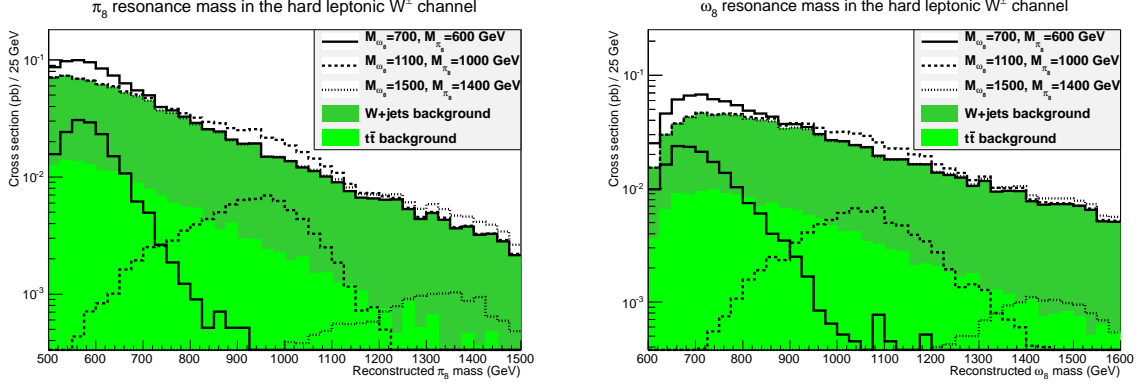


FIG. 5: Invariant mass distributions for the reconstructed π_8 and ω_8 for a few sample mass points in the hard leptonic W channel (see the text for details). The ω_8 decay constant parameter ξ is set to 0.2, in order to make the curves clearly distinguishable on top of the backgrounds.

to a hadronic W , which still gives significant reduction of the main $W + \text{jets}$ background. As in the previous case, the main backgrounds are $W + \text{jets}$ and semileptonically decaying $t\bar{t}$. The cuts used in this case are:

- Exactly 1 isolated lepton with $p_\perp > 50$ GeV;
- Missing $E_T > 50$ GeV;
- A reconstructed leptonic W_{lep} with $p_\perp > 200$ GeV;
- A jet j_1 with $p_\perp > 200$ GeV;
- Invariant mass (reconstructed π_8 mass) $M(W_{\text{lep}}, j_1) > 500$ GeV;
- A hadronic W reconstructed from two non-leading jets with $p_\perp > 20$ GeV, with the invariant mass between 50 and 110 GeV.

Details about leptonic W reconstruction are given in Sec. III A. If multiple hadronic W candidates are found within the required invariant mass window, the candidate with mass closest to the W mass is selected. The energy of the hadronic W is rescaled to get the correct W mass, keeping η , ϕ and p_\perp fixed, before reconstruction of the ω_8 from the reconstructed π_8 momentum and the hadronic W .

Fig. 5 shows the reconstructed π_8 and ω_8 invariant mass distributions for a few different $(m_{\omega_8}, m_{\pi_8})$ mass points (using $\xi = 0.2$), together with the main backgrounds. The invariant mass widths are slightly larger than those in the “hard W jet” case, due to the larger energy scale

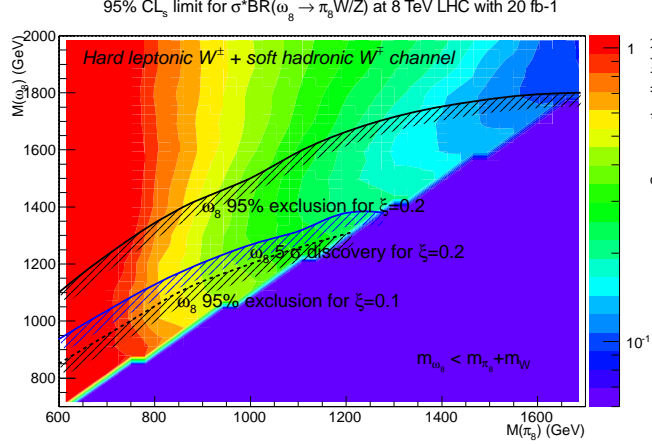


FIG. 6: Cross section exclusion limits in pb in the (ω_8, π_8) mass plane in the hard leptonic W channel, for 20 fb^{-1} integrated luminosity at the 8 TeV LHC. Also the exclusion regions for ω_8 with ξ set to 0.1 and 0.2 are indicated.

uncertainty of the missing E_T , as well as the combinatoric uncertainty for selecting among possible hadronic W candidates. We again use the reconstructed π_8 “bump” to determine the exclusion and discovery limits.

Fig. 6 shows the 95% cross section exclusion contours for 20 fb^{-1} at the 8 TeV LHC, as well as the exclusion curves for ω_8 production with two different values of ξ , 0.1 and 0.2, assuming $\mathcal{B}(\omega_8 \rightarrow \pi_8^\pm W^\mp) = 2/3$ and $\mathcal{B}(\omega_8 \rightarrow \pi_8^0 Z) = 1/3$. The exclusion reach for this channel is, as expected, not as good as that for the hard W -tagged jet channel described in the previous case (extending to m_{ω_8} near 1300 GeV for $\xi = 0.1$ and m_{ω_8} around 1800 GeV for $\xi = 0.2$), but it can still be interesting as a cross-check. For a 5σ discovery in this channel, the ω_8 mass must be below 1380 GeV assuming $\xi = 0.2$. As for $\xi = 0.1$, no discovery is possible in the studied mass region.

C. Soft leptonic Z with a hard Z jet

Since we assume the ω_8 decay to be isospin invariant, we expect $1/3$ of the events to feature $\omega_8 \rightarrow \pi_8^0 + Z$. This channel might seem promising *a priori*, thanks to the excellent invariant mass reconstruction of a leptonically decaying Z boson, as well as the lower backgrounds. Here the $t\bar{t}$ background is negligible if a lepton pair is required to be close to the Z mass and an upper limit on missing E_T is imposed. However, the smaller cross section for Z +jets production compared to W +jets production for the background is balanced by several factors. These include a considerably smaller, roughly a factor three, branching ratio into e and μ , the factor two smaller ω_8 decay rate,

together with slightly worse cut efficiencies (since, e.g., two isolated leptons are required). Due to these factors, the Z decay mode overall has a three times worse cross section exclusion than the W mode, and will therefore not be relevant for an exclusion or discovery study. But it would certainly be important in a later stage, after discovery of a signal, to establish the isospin symmetry of the ω_8 decays.

For completeness, here we list the cuts used in our analysis:

- Exactly 2 isolated same-flavor opposite-sign leptons (e or μ) with $p_\perp > 20$ GeV and an invariant mass $|M(l^+, l^-) - m_Z| < 15$ GeV;
- Missing $E_T < 50$ GeV;
- A W -tagged jet j_Z (with mass range centered around m_Z) with $p_\perp > 200$ GeV;
- A jet j_1 with $p_\perp > 200$ GeV;
- Invariant mass (reconstructed π_8 mass) $M(j_Z, j_1) > 500$ GeV.

IV. CONCLUSIONS AND DISCUSSIONS

In this article, we have studied search prospects and the phenomenology of doubly resonant signals which result from the decay of a neutral $SU(2)_L$ singlet color-octet vector state ω_8 into a lighter $SU(2)_L$ triplet color-octet scalar π_8 . While these type of resonances have been subject of extensive collider studies, they have been mostly studied individually.

It should be noted that such color-octet resonances often come together in various $SU(2)_L$ representations, which give rise to doubly resonant signals. Assuming $m_{\omega_8} > m_{\pi_8} + m_W$, we have provided the search prospects and phenomenology of $\omega \rightarrow \pi_8^\pm W^\mp (\pi_8^0 Z) \rightarrow gW^\pm W^\mp (gZZ)$ signature. We find that the signal can be efficiently excluded, and even discovered, for a large range of masses and parameter choices, already for the present 8 TeV run of the LHC. The most effective search channel is for π_8 decaying into a boosted W boson that decays hadronically, plus a hard gluon jet, while the W from the ω_8 decay goes into a lepton and missing transverse energy. This channel gives at the same time excellent background suppression and superior resolution in the mass peak reconstruction. Furthermore, for this channel, the dominant SM background is W + jets production, where a hard jet is falsely tagged as a W jet. For this channel, it might be possible to further improve the signal significance by using more complicated multivariable W jet tagging methods, as described in Ref. [29].

Our analysis demonstrates how a sizable branching fraction for $\omega_8 \rightarrow \pi_8 W$ (rather than dominantly decaying into $q\bar{q}$) allows access to two resonances in one stroke. This is clearly advantageous compared to the case where π_8 has to be produced in pairs in strong interaction, making it inaccessible at the early run at 8 TeV, in particular when the resonances have masses around or above TeV.

Acknowledgments. The authors would like to thank Kai-Feng Chen for useful discussions and patient help with the code for the CL_s method. H.Y. thanks KEK Theory Center for the hospitality during his stay which was made possible by the exchange program between KEK Theory Center and NCTS in Taiwan. J.A. is supported by NTU Grant No. 10R1004022, T.E. and H.Y. are supported in part by the National Science Council of Taiwan under Grant No. NSC 100-2119-M-002-061 and NSC 100-2119-M-002-001. W.-S.H. thanks the National Science Council for Academic Summit grant NSC 100-2745-M-002-002-ASP.

-
- [1] P.H. Frampton and S.L. Glashow, Phys. Lett. B **190**, 157 (1987).
 - [2] J. Bagger, C. Schmidt and S. King, Phys. Rev. D **37**, 1188 (1988).
 - [3] H. Davoudiasl, J.L. Hewett and T.G. Rizzo, Phys. Rev. D **63**, 075004 (2001).
 - [4] B. Lillie, L. Randall and L.-T. Wang, JHEP **0709**, 074 (2007).
 - [5] T. Appelquist, H.-C. Cheng and B.A. Dobrescu, Phys. Rev. D **64**, 035002 (2001).
 - [6] J.L. Hewett and T.G. Rizzo, Phys. Rept. **183**, 193 (1989).
 - [7] I. Dorsner and P. Fileviez Perez, Nucl. Phys. B **723**, 53 (2005).
 - [8] U. Baur, I. Hinchliffe and D. Zeppenfeld, Int. J. Mod. Phys. A **2**, 1285 (1987).
 - [9] U. Baur, M. Spira and P.M. Zerwas, Phys. Rev. D **42**, 815 (1990).
 - [10] See for example S.P. Martin, In *Kane, G.L. (ed.): Perspectives on supersymmetry II* 1-153 [hep-ph/9709356].
 - [11] R.S. Chivukula, R. Rosenfeld, E.H. Simmons and J. Terning, In *Barklow, T.L. (ed.) et al.: Electroweak symmetry breaking and new physics at the TeV scale* 352-382 [hep-ph/9503202].
 - [12] C.T. Hill, Phys. Lett. B **266**, 419 (1991).
 - [13] C.T. Hill and S.J. Parke, Phys. Rev. D **49**, 4454 (1994).
 - [14] T. Han, I. Lewis and Z. Liu, JHEP **1012**, 085 (2010).
 - [15] K. Ishiwata and M.B. Wise, Phys. Rev. D **83**, 074015 (2011).
 - [16] T. Enkhbat, W.-S. Hou and H. Yokoya, Phys. Rev. D **84**, 094013 (2011).
 - [17] B. A. Dobrescu, K. Kong and R. Mahbubani, Phys. Lett. B **670**, 119 (2008).
 - [18] Y. Bai and A. Martin, Phys. Lett. B **693**, 292 (2010).

- [19] S. Schumann, A. Renaud and D. Zerwas, JHEP **1109**, 074 (2011).
- [20] B.A. Dobrescu and G.Z. Krnjaic, Phys. Rev. D **85**, 075020 (2012).
- [21] Y. Kats and M. J. Strassler, arXiv:1204.1119 [hep-ph].
- [22] CMS-PAS-EXO-12-016, [CMS collaboration] (2012).
- [23] ATLAS-CONF-2012-088, [ATLAS collaboration] (2012).
- [24] G. Aad *et al.* [ATLAS Collaboration], arXiv:1207.2409 [hep-ex].
- [25] S. Chatrchyan *et al.* [CMS Collaboration], arXiv:1207.1798 [hep-ex].
- [26] S. Chatrchyan *et al.* [CMS Collaboration], arXiv:1207.1898 [hep-ex].
- [27] G. Aad *et al.* [ATLAS Collaboration], arXiv:1207.4686 [hep-ex].
- [28] J.M. Butterworth, A.R. Davison, M. Rubin and G.P. Salam, Phys. Rev. Lett. **100**, 242001 (2008).
- [29] Y. Cui, Z. Han and M.D. Schwartz, Phys. Rev. D **83**, 074023 (2011).
- [30] A. Altheimer, S. Arora, L. Asquith, G. Brooijmans, J. Butterworth, M. Campanelli, B. Chapleau and A.E. Cholakian *et al.*, J. Phys. G **39**, 063001 (2012).
- [31] L. D. Landau, Dokl. Akad. Nauk., USSR **60**, 207 (1948); C. -N. Yang, Phys. Rev. **77**, 242 (1950).
- [32] J. Pumplin, D.R. Stump, J. Huston, H.-L. Lai, P.M. Nadolsky and W.-K. Tung, JHEP **0207**, 012 (2002).
- [33] CMS PAS-JME-10-013, [CMS Collaboration].
- [34] G. Aad *et al.* [ATLAS Collaboration], arXiv:1206.5369 [hep-ex].
- [35] S.D. Ellis, C.K. Vermilion and J.R. Walsh, Phys. Rev. D **80**, 051501 (2009).
- [36] A.L. Read, In *Geneva 2000, Confidence limits* 81-101.
- [37] L. Moneta, K. Belasco, K.S. Cranmer, S. Kreiss, A. Lazzaro, D. Piparo, G. Schott and W. Verkerke *et al.*, PoS ACAT **2010**, 057 (2010) [arXiv:1009.1003 [physics.data-an]].
- [38] J. Alwall, M. Herquet, F. Maltoni, O. Mattelaer and T. Stelzer, JHEP **1106**, 128 (2011).
- [39] T. Sjostrand, S. Mrenna and P.Z. Skands, JHEP **0605**, 026 (2006).
- [40] S. Ovnyn, X. Rouby and V. Lemaitre, arXiv:0903.2225 [hep-ph].
- [41] C. Degrande, C. Duhr, B. Fuks, D. Grellscheid, O. Mattelaer and T. Reiter, Comput. Phys. Commun. **183**, 1201 (2012).
- [42] J. Alwall, S. de Visscher and F. Maltoni, JHEP **0902**, 017 (2009).
- [43] M. Cacciari, G.P. Salam and G. Soyez, JHEP **0804**, 063 (2008).
- [44] M. Cacciari, G.P. Salam and G. Soyez, Eur. Phys. J. C **72**, 1896 (2012).